Dalton Transactions

ROYAL SOCIETY OF CHEMISTRY

COMMUNICATION

Cite this: *Dalton Trans.*, 2024, **53**, 19116

Received 22nd October 2024,
Accepted 12th November 2024

DOI: 10.1039/d4dt02953d

rsc.li/dalton

Rim-brominated pillarplexes and their assembly *via* self-sorting†

Julian Zuber, [a] Thomas Pickl, [a] Alexandra A. Heidecker, [a] Marco Baron, [b] Christian Jandl [c] and Alexander Pöthig *[a]

We report rim-brominated pillarplexes, new examples of functionalised supramolecular organometallic complexes (SOCs). The bromide atoms can be introduced to the established pristine ligand precursor, demonstrating late-stage diversification of our ligand platform. SC-XRD/ED-derived crystal structures of precursor and pillarplex salts are reported along with competitive assembly experiments of the Ag(I) pillarplex, showing narcissistic self-sorting behavior.

Self-assembly and self-sorting are two fundamental phenomena observed and employed in supramolecular chemistry.[1] In nature, highly sophisticated self-assembly processes can be observed, such as DNA double helix formation or the folding of polypeptides into proteins, which show exceptional selectivity *via* self-sorting.[2] In less complex synthetic systems, self-sorting has also been exploited[1] and can be controlled thermodynamically or kinetically.[3] In this context, narcissistic self-sorting refers to the self-recognition of identical molecular building blocks and their mutual affinity. In contrast, social self-sorting describes the attraction between mostly very different molecular species.[1,3] In metallosupramolecular assemblies the combination of suitable metals with polydentate ligands can lead to several homo- or heteroleptic arrangements.[4–6] Such architectures have also been achieved by high-fidelity self-sorting of geometrically different ligand scaffolds pioneered by the groups of Lehn,[7] Raymond,[8] Stang,[9] Nitschke[10] and Fujita.[11] More recently, self-sorting phenomena were transferred to supramolecular organometallic complexes (SOCs).[3,12,13] In 2016, our group introduced a subclass of SOCs, so-called pillarplexes $\mathbf{M_8L_2(X)_4}$ (M = Ag, Au; X = OTf, PF_6, OAc).[14] These are octanuclear metal–NHC complexes forming metallocavitand structures with tubular cavities.[15] We also demonstrated that modification of the macrocyclic ligands by introduction of triazole moieties leads to rim-modified pillarplexes and enables structural alignments as well as self-recognition of the SOCs in the solid state.[16] However, this strategy required a *de novo* synthesis of the whole macrocycle. Herein, we now report a late-stage bromide-functionalisation of our macrocyclic pillarplex proligand $\mathbf{H_6L(X)_4}$ (**X** = OTf, PF_6) – without the necessity to construct the entire macrocycle *de novo*. The self-assembly of brominated ligands using coinage metal ions Ag(I) and Au(I) leads to the respective rim-brominated pillarplexes (Fig. 1, top). Competitive experiments towards ligand exchange reactions (pristine *vs.* brominated ligand) enabled by the labile Ag–NHC bond,[17] show the highly preferred formation of the homoleptic rim-brominated pillarplex although a statistical distribution might be expected due to only peripheral differences in the ligand scaffold (Fig. 1, bottom).

Aiming to construct modified pillarplexes, we first targeted the synthesis of calix[4]imidazolium[2]dibromo-pyrazole proligands $\mathbf{H_6L^{Br2}(X)_4}$ (**X** = OTf, PF_6), starting from previously

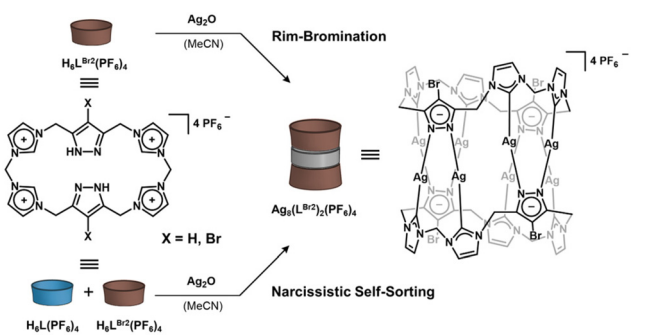

Fig. 1 Formation of the rim-brominated pillarplex $\mathbf{Ag_8(L^{Br2})_2(PF_6)_4}$ *via* self-assembly and narcissistic self-sorting.

[a]*Catalysis Research Center & Department of Chemistry, Technische Universität München, Ernst-Otto-Fischer Str. 1, 85748 Garching bei München, Germany. E-mail: alexander.poethig@tum.de*
[b]*Dipartimento di Scienze Chimiche, Università degli Studi di Padova, via Marzolo 1, 35131 Padova, Italy*
[c]*ELDICO Scientific AG, Switzerland Innovation Park Basel Area, Hegenheimermattweg 167A, 4123 Allschwil, Switzerland*

† Electronic supplementary information (ESI) available. CCDC 2374510–2374513. For ESI and crystallographic data in CIF or other electronic format see DOI: https://doi.org/10.1039/d4dt02953d

reported pristine proligands $H_6L(X)_4$.[18] Bromine functionalisation was achieved by slow addition of *N*-bromosuccinimde (NBS) to a solution of the respective $H_6L(X)_4$ salt in acetonitrile (MeCN) (Scheme 1). The reaction likely follows an electrophilic substitution mechanism at the pyrazole C–H backbone due to the polar solvent.[19] Evidently, the bromination rate is influenced by the choice of counterions. In presence of triflate (OTf) anions, elevated temperatures (*i.e.* 40 °C for 24 h) are required, while in case of hexafluorophosphate (PF_6), full conversion of the starting material is observed after one hour at room temperature. A possible explanation might be the slightly increased solubility of $H_6L(PF_6)_4$ over $H_6L(OTf)_4$ in acetonitrile. Metalation with Ag_2O cleanly yielded $Ag_8(L^{Br2})_2(PF_6)_4$ and subsequent transmetalation with Au(THT)Cl (chloro(tetrahydrothiophene)gold(I)) afforded $Au_8(L^{Br2})_2(PF_6)_4$ according to established protocols.[14] The molecular structures of the ligand precursors as well as pillarplexes were determined by single-crystal X-ray diffraction (SC-XRD) ($H_6L^{Br2}(PF_6)_4$, $Ag_8(L^{Br2})_2(PF_6)_4$, $Au_8(L^{Br2})_2(PF_6)_4$) and electron diffraction (ED) ($H_6L^{Br2}(OTf)_4$). Suitable crystalline samples were obtained by diffusion of diethyl ether (Et_2O) into solutions of MeCN. Whereas $H_6L^{Br2}(OTf)_4$ crystallises in the orthorhombic space group *Pbca* (no. 61) (see ESI Fig. S45†), ligand precursor $H_6L^{Br2}(PF_6)_4$ crystallises in the monoclinic space group *C*2/*c* (no. 15) (see ESI Fig. S46†). Despite the limited quality of the crystal and resulting data (for details see ESI†), the crystal structure serves as evidence for the connectivity and illustrates an unstrained conformation of the ligand where the opposing bromine atoms are pointing towards antiparallel directions, likely due to their steric demand. $Ag_8(L^{Br2})_2(PF_6)_4$ crystallises in the orthorhombic space group *Pnma* (no. 62) and $Au_8(L^{Br2})_2(PF_6)_4$ in the tetragonal space group $P4_12_12$ (no. 92).

The molecular compositions comprising eight metal atoms coordinated by two octadentate NHC ligands are identical to the pristine pillarplexes showing reasonably similar geometries and also exhibiting intramolecular metallophilic contacts (Fig. 2).[14] With respect to the pore, the brominated congeners exhibit a slightly larger opening than the pristine and triazolate pillarplexes.[14,16] For the latter, we had shown that the rim modification results in a more flexible pore. In the brominated case, this trend is now reversed, with a larger energetic penalty for smaller portals as derived by DFT calculations (see ESI†). It is noteworthy that residual (solvent molecule) electron density was found in the pores of the cavitand which could not be refined explicitly (see ESI†). The packing reveals an alignment of the $Ag_8(L^{Br2})_2(PF_6)_4$ pores (ESI Fig. S48†), in which the cationic pillarplexes stack on top of each other along the crystallographic *c*-axis, surrounded by the counterions. In contrast, in $Au_8(L^{Br2})_2(PF_6)_4$, the cations stack on top of each other in an alternating manner without any pore alignment (ESI Fig. S51†). Here, the PF_6 counterions occupy the space between the alternating pillarplex pores, preventing channel formation along the crystallographic *c*-axis.

With both the pristine and brominated ligand precursors prepared, we sought to determine whether the metal–ligand bonds in derived pillarplexes exhibited the dynamic nature commonly observed in Ag–NHC bonds.[17] To explore this, we conducted a competitive experiment to identify potential self-sorting behaviour. Therefore, we investigated the metalation of mixtures of pristine and brominated ligand using the literature-known procedure to self-assemble Ag(I) pillarplexes (Fig. 3a).[14] The reactions were monitored after different reaction times and temperatures by ^{1}H NMR spectroscopy and HRESI-MS to identify the formed species. Owing to the characteristic isotopic ratios of Br and Ag, the different homo- and heteroleptic pillarplex species as well as the precursors can be unequivocally identified in the mass spectra (Fig. 3d). In case

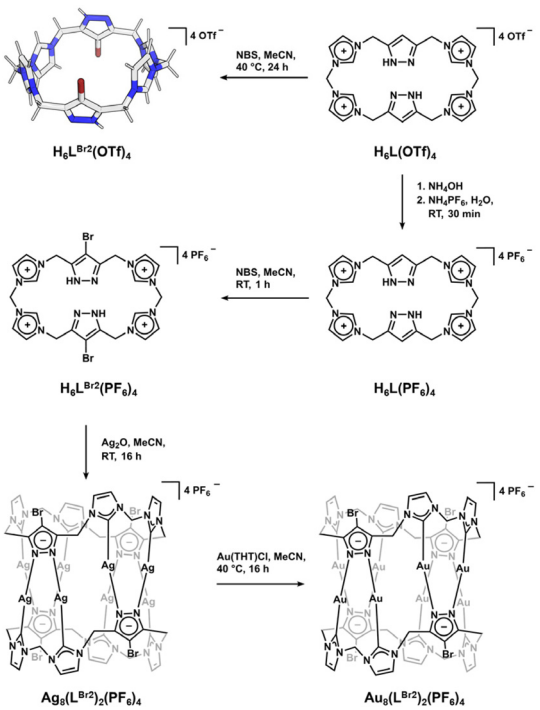

Scheme 1 Synthesis of ligand precursor $H_6L^{Br2}(PF_6)_4$ and $H_6L^{Br2}(OTf)_4$ (ED structure) and the self-assembly of functionalised pillarplexes $Ag_8(L^{Br2})_2(PF_6)_4$ and $Au_8(L^{Br2})_2(PF_6)_4$.

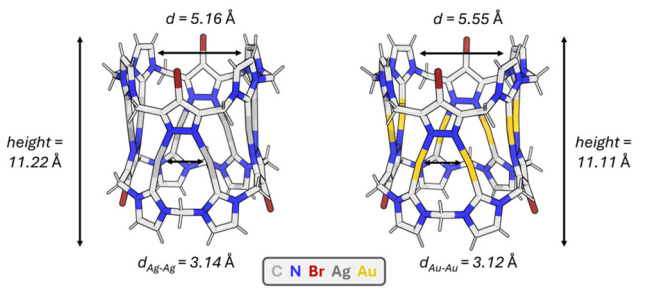

Fig. 2 Molecular structures of the cations of $Ag_8(L^{Br2})_2(PF_6)_4$ and $Au_8(L^{Br2})_2(PF_6)_4$. Counterions, solvent molecules and disorders are omitted for clarity. The distance *d* corresponds to the pore opening as defined in the ESI.†

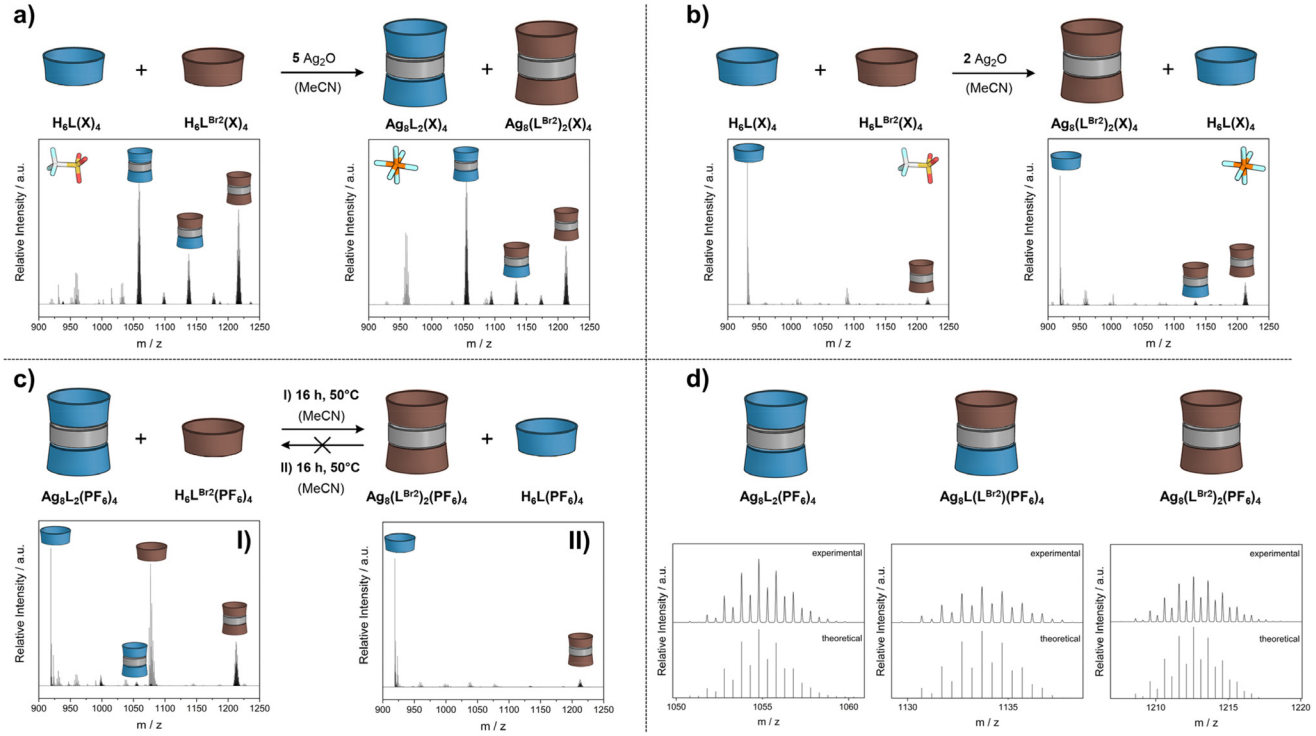

Fig. 3 Graphical representation of self-sorting experiments with the respective HRESI-MS spectra: (a) equimolar amounts of the ligands were reacted with 5 equivalents of Ag_2O at room temperature in MeCN. The mass spectra show the result of the reaction with OTf as counterion (left) and PF_6 anion (right) after 16 h at room temperature. (b) The same reaction is shown but with insufficient amounts of Ag_2O (2 equiv.). (c) The reaction of $\mathbf{Ag_8L_2(PF_6)_4}$ with 5 equivalents of $\mathbf{H_6L^{Br2}(PF_6)_4}$ (I), the reversed reaction, where $\mathbf{Ag_8(L^{Br2})_2(PF_6)_4}$ was reacted with excess of $\mathbf{H_6L(PF_6)_4}$ (5 equiv.) (II), and their HRESI-MS spectra after 16 h at 50 °C are depicted. (d) The experimental and theoretical isotopic patterns of $\mathbf{[Ag_8L_2(PF_6)_2]^{2+}}$, $\mathbf{[Ag_8L(L^{Br2})(PF_6)_2]^{2+}}$ and $\mathbf{[Ag_8(L^{Br2})_2(PF_6)_2]^{2+}}$ are illustrated.

of $\mathbf{H_6L^{Br2}(PF_6)_4}$ and $\mathbf{H_6L(PF_6)_4}$, the formation of homoleptic species is preferred over that of the heteroleptic pillarplex after 16 h at room temperature with 5 equivalents of Ag_2O, resembling a preference for narcissistic self-sorting without statistical distribution which could be expected. Longer reaction times up to 96 h resulted in no observable changes in the distribution, suggesting that ligand exchange reactions do not occur once the respective pillarplex is assembled. Increasing the reaction temperature (*i.e.* 50 °C) or the excess of Ag_2O (*i.e.* 15 equiv.) resulted in the same behaviour, however the ratio of the species slightly changed in favour of the heteroleptic pillarplex. Since the counterions can have a significant impact on the self-sorting behaviour,[20] we repeated the self-assembly experiments with the triflate salts. As a result, both homoleptic species were detected, along with small amounts of the heteroleptic species, which showed only a slight increase compared to the PF_6 experiment. In an additional competitive experiment we added sub-stoichiometric amounts of Ag_2O to a solution of equimolar amounts of $\mathbf{H_6L^{Br2}(X)_4}$ and $\mathbf{H_6L(X)_4}$ in CD_3CN (Fig. 3b). Regardless of the counterion in this setting, the brominated precursors $\mathbf{H_6L^{Br2}(X)_4}$ were completely converted to the respective pillarplexes $\mathbf{Ag_8(L^{Br2})_2(X)_4}$, whereas no pristine pillarplexes $\mathbf{Ag_8L_2(X)_4}$ formed by reaction of the unsubstituted ligand precursors in spite of the same coordination geometry. In a second experiment (Fig. 3c, **I**), we added an excess of brominated precursor $\mathbf{H_6L^{Br2}(PF_6)_4}$ (5 equiv.) to a solution of unsubstituted pillarplex $\mathbf{Ag_8L_2(PF_6)_4}$ in CD_3CN, which led to nearly quantitative conversion of the pristine pillarplex to the brominated congener $\mathbf{Ag_8(L^{Br2})_2(PF_6)_4}$ after 16 h at 50 °C, accompanied by quantitative release of $\mathbf{H_6L(PF_6)_4}$. Adding sodium acetate as an additional base facilitates this exchange to be completed already after 16 h at ambient temperature (see ESI Fig. S33†). In a third (reversed) setting, we added an excess of pristine ligand $\mathbf{H_6L(PF_6)_4}$ to a solution of brominated pillarplex $\mathbf{Ag_8(L^{Br2})_2(PF_6)_4}$ in CD_3CN (Fig. 3c, **II**). In this case, hardly any conversion was observed. Only traces of pristine pillarplex and heteroleptic species could be detected after 16 h of reaction at 50 °C. Moreover, here, the presence of NaOAc as additional base did not have a significant impact on the reaction outcome (see ESI Fig. S35†). The results of these three experiments further support the preferred narcissistic self-sorting behaviour during the pillarplex assembly. Additionally, the brominated pillarplex appears to be the favoured product of both possible homoleptic species, which we attribute to thermodynamic reasons. In particular, the last two experiments (Fig. 3c) strongly indicate that a ligand exchange in principle is possible, which is expected due to the labile nature of the Ag–NHC bond.[17,21] However, only the pristine pillarplex is converted, whereas the brominated pillarplex shows no back reaction.

DFT calculations support this thermodynamic preference, as the formation of brominated pillarplex *via* a ligand exchange reaction from the pristine congener was calculated to be exergonic (see ESI†). Accordingly, the negative ΔG is both caused by enthalpic (ΔH_R = −31.2 kJ mol^{-1}) and/or entropic factors ($T\Delta S_R$ = −12.4 kJ mol^{-1}): Given that the coordination geometries of both the homoleptic pristine and the brominated pillarplex (both point group D_{2d}) are almost identical, we hypothesise that the enthalpic contribution is likely induced by electronic effects of the bromide substitution, *i.e.* by strengthening the coordination bond *e.g.* by the +M effect of the bromide ligand. An entropic preference could be caused by the difference towards the reduction of the rotational freedom of the ligand (precursor) upon coordination. In this case a more flexible ligand precursor would exhibit a stronger entropic penalty upon being "locked" into the staggered conformation within the pillarplex. Likewise, if the macrocyclic ligand precursor were less flexible, *e.g.* due to the newly introduced bromine substituent, the entropic penalty of the locking would be smaller. To experimentally test this hypothesis, we conducted variable-temperature NMR (VT-NMR) experiments in CD_3CN with $\mathbf{H_6L(PF_6)_4}$ and $\mathbf{H_6L^{Br2}(PF_6)_4}$. Less pronounced broadening and splitting of signal sets in the ^{1}H NMR spectrum or lower coalescence temperatures are concomitant with a higher rotational flexibility and lower energy barriers during the rotation.[22] In fact, $\mathbf{H_6L(PF_6)_4}$ (see ESI Fig. S19a†) shows sharp singlets in the ^{1}H NMR spectrum and only the imidazolium backbone signals at 7.64 ppm and 7.50 ppm are split into two virtual triplets which coalesce into a broad singlet at elevated temperature (see ESI Table S1†). The NH protons are not observable likely due to proton exchange with the deuterated solvent. For $\mathbf{H_6L^{Br2}(PF_6)_4}$ (see ESI Fig. S19b†), the signals at 5.42 ppm (CH_2), 7.49 ppm (NCHC), 8.78 ppm (NCHN) and 11.87 ppm (NH) are split and coalesce over a broad temperature range (see ESI Table S1†). As a result, we conclude a lower rotational flexibility of the brominated proligand $\mathbf{H_6L^{Br2}(PF_6)_4}$ where each conformation change consumes more energy as in the pristine congener. Therefore, the entropic penalty for the coordination can be expected to be lower for $\mathbf{H_6L^{Br2}(PF_6)_4}$.

In summary, we successfully synthesised a functionalised calix[4]imidazolium[2]pyrazole cyclophane by late-stage introduction of bromine substituents. This ligand serves as precursor for the corresponding rim-brominated Ag(I) and Au(I) pillarplexes. The crystal structures of all compounds showed the same general structural features as the pristine pillarplexes. Pore openings and height changed according to the steric demand of the bromine atoms. In competitive experiments, strong preferences for narcissistic self-sorting were observed. Regardless of the counterion and despite almost identical ligand geometries, functionalised pillarplex $\mathbf{Ag_8(L^{Br2})_2(X)_4}$ is preferably formed over pristine pillarplex $\mathbf{Ag_8L_2(X)_4}$. Addition of an excess of functionalised ligand $\mathbf{H_6L^{Br2}(PF_6)_4}$ to the pristine pillarplex $\mathbf{Ag_8L_2(PF_6)_4}$ led to a nearly quantitative conversion to $\mathbf{Ag_8(L^{Br2})_2(PF_6)_4}$, while completely liberating $\mathbf{H_6L(PF_6)_4}$. NaOAc heavily accelerates this exchange by deprotonation of free ligand $\mathbf{H_6L^{Br2}(PF_6)_4}$. In the reversed experimental configuration, addition of $\mathbf{H_6L(PF_6)_4}$ to $\mathbf{Ag_8(L^{Br2})_2(PF_6)_4}$ resulted in negligible reactivity, despite the presence of NaOAc as an additive. This behaviour suggests a higher affinity for the formation of brominated pillarplexes, which may be attributed to enthalpic and/or entropic factors. This enhanced affinity may result from stronger coordination interactions due to the bromide substitution, potentially altering the electronic properties of the ligand. Additionally, differences in ligand flexibility between the brominated and pristine variants could lead to varying entropic penalties upon complex formation, contributing to the observed preferential binding. These results render the functionalised cyclophanes and pillarplexes interesting building blocks for more complex platforms accessible *via* self-assembly or materials based on self-sorting phenomena. Based on these seminal results, we aim to expand the scope of the rim-functionalisation of pillarplexes towards a more comprehensive understanding of the self-sorting phenomenon, allowing to explore new avenues for different applications.

Author contributions

J. Z.: investigation (lead), data curation (lead), visualisation (lead), formal analysis (lead), and writing – original draft; T. P.: data curation, formal analysis, and writing – review & editing; A. A. H.: investigation, and formal analysis; M. B.: investigation; C. J.: formal analysis; A. P.: conceptualisation, resources, funding acquisition, methodology, project administration, supervision, validation, and writing – review & editing.

Data availability

The data supporting this article have been included as part of the ESI.†

Conflicts of interest

There are no conflicts to declare.

Acknowledgements

This work is financed by the Deutsche Forschungsgemeinschaft (DFG, German Research Foundation) – Project SPP 1928 (project 434509373). T.P. thanks the Studienstiftung des deutschen Volkes for funding this work. We also very much acknowledge Technical University of Munich (Catalysis Research Center, Department of Chemistry, Graduate School) for financial support.

References

1 M. M. Safont-Sempere, G. Fernandez and F. Würthner, *Chem. Rev.*, 2011, **111**, 5784–5814.

2 J. D. Watson and F. H. C. Crick, *Nature*, 1953, **171**, 737–738.
3 N. Sinha, T. T. Y. Tan, E. Peris and F. E. Hahn, *Angew. Chem., Int. Ed.*, 2017, **56**, 7393–7397.
4 J. E. M. Lewis, A. Tarzia, A. J. P. White and K. E. Jelfs, *Chem. Sci.*, 2019, **11**, 677–683.
5 R. J. Li, A. Tarzia, V. Posligua, K. E. Jelfs, N. Sanchez, A. Marcus, A. Baksi, G. H. Clever, F. Fadaei-Tirani and K. Severin, *Chem. Sci.*, 2022, **13**, 11912–11917.
6 L. S. Lisboa, J. A. Findlay, L. J. Wright, C. G. Hartinger and J. D. Crowley, *Angew. Chem., Int. Ed.*, 2020, **59**, 11101–11107.
7 R. Krämer, J.-M. Lehn and A. Marquis-Rigault, *Proc. Natl. Acad. Sci. U. S. A.*, 1993, **90**, 5394–5398.
8 D. L. Caulder and K. N. Raymond, *Angew. Chem., Int. Ed.*, 2003, **36**, 1440–1442.
9 Y.-R. Zheng, H.-B. Yang, B. H. Northrop, K. Ghosh and P. J. Stang, *Inorg. Chem.*, 2008, **47**, 4706–4711.
10 V. E. Campbell, X. de Hatten, N. Delsuc, B. Kauffmann, I. Huc and J. R. Nitschke, *Nat. Chem.*, 2010, **2**, 684–687.
11 Q.-F. Sun, J. Iwasa, D. Ogawa, Y. Ishido, S. Sato, T. Ozeki, Y. Sei, K. Yamaguchi and M. Fujita, *Science*, 2010, **328**, 1144–1147.
12 A. Pöthig and A. Casini, *Theranostics*, 2019, **9**, 3150–3169.
13 S. Ibanez, M. Poyatos and E. Peris, *Acc. Chem. Res.*, 2020, **53**, 1401–1413.
14 P. J. Altmann and A. Pöthig, *J. Am. Chem. Soc.*, 2016, **138**, 13171–13174.
15 P. J. Altmann and A. Pöthig, *Angew. Chem., Int. Ed.*, 2017, **56**, 15733–15736.
16 S. Guan, T. Pickl, C. Jandl, L. Schuchmann, X. Zhou, P. J. Altmann and A. Pöthig, *Org. Chem. Front.*, 2021, **8**, 4061–4070.
17 H. M. J. Wang and I. J. B. Lin, *Organometallics*, 1998, **17**, 972–975.
18 P. J. Altmann, C. Jandl and A. Pöthig, *Dalton Trans.*, 2015, **44**, 11278–11281.
19 M. C. Carreño, J. L. Garcia Ruano, G. Sanz, M. A. Toledo and A. Urbano, *J. Org. Chem.*, 1995, **60**, 5328–5331.
20 X. Zhao, H. Wang, B. Li, B. Zheng, D. Yang, W. Xu, X. Li, X. J. Yang and B. Wu, *Chem. Commun.*, 2021, **57**, 6078–6081.
21 R. C. Nishad and A. Rit, *Chem. – Eur. J.*, 2021, **27**, 594–599.
22 M. T. Huggins, T. Kesharwani, J. Buttrick and C. Nicholson, *J. Chem. Educ.*, 2020, **97**, 1425–1429.